Qualification of the T6 Ion Thruster for the BepiColombo Mission to the Planet Mercury

IEPC-2011-234

Presented at the 32nd International Electric Propulsion Conference,
Wiesbaden • Germany
September 11 – 15, 2011

Dr. Angelo N. Grubisic[1]

Flux Engineering Ltd., Farnborough, Hampshire, GU14 0LX, United Kingdom

Stephen Clark[2] and Neil Wallace[3]
QinetiQ Space Division, Farnborough, Hampshire, United Kingdom

Dr. C Collingwood[4] and Francesco Guarducci[4]

University of Southampton/Mars Space, Southampton, Hampshire, SO17 1BJ, United Kingdom

Abstract: This paper describes the system element and architecture of the Solar Electric Propulsion System (SEPS) for the BepiColombo mission to Mercury and the approach to qualification of the Solar Electric Propulsion Thruster (SEPT). The respective system architecture for the SEPS is described together with the qualification programmes underway. The SEPS required for inter-planetary cruise benefits from its wide operating range, robust design and its ability to be easily adaptable to a wide range of platforms and applications. Critical to the SEPS system design is the redundancy and cross-strapping philosophy. The selected configuration of two PPUs with fully symmetric cross-strapping of T6 units to PPU outputs gains maximum benefit from the symmetry of the four engine configuration. The resulting design provides for an elegant AIV sequence and plan. The number of PPU units is minimized and mounting/demounting units is straightforward and the number of operating modes for testing and characterization is minimized. The approach to qualification of the SEPT is described, as developed through Assembly, Integration and Verification (AIV) activities leading up to the BepiColombo mission, including; mechanical integrity, Thermal Vacuum (TV), Electromagnetic Compatibility (EMC), Electromagnetic Interference (EMI) and thrust performance characterization as well as the development of the necessary Ground Support Equipment (GSE). Performance verification of a fully representative SEPS is considered to be an essential element in the qualification of the SEPT.

[1] Director/Propulsion Systems Engineer, Flux Engineering Ltd., A.Grubisic@Flux-Engineering.com
[2] AIV Team Leader, QinetiQ Space Division, SDClark1@QinetiQ.com
[3] Chief Engineer, QinetiQ Space Division, NCWallace@QinetiQ.com
[4] Research Eng., Mars Space, Cheryl.Collingwood@Mars-Space.co.uk, Francesco.Guarducci@mars-space.co.uk

I. Introduction

THE BepiColombo mission[1] to Mercury, due to launch in 2014, provides Europe with unique technical challenges. The spacecraft will fly in a trajectory that comes closer to the sun than any previous mission, carrying the largest solar electric propulsion system (SEPS) of its kind ever flow in Europe. The SEPS will provide the necessary impulse during the inter-planetary cruise with each thruster delivering a total impulse requirement of 11.7MNs.

The SEPS consists of four 22-cm T6 Solar Electric Propulsion Thrusters (SEPT), each of which is capable of throttling between 40 – 145 mN; four Flow Control Units (FCU) dedicated to an associated SEPT; two Power Processing Units (PPU), each of which is comprised of 2-sets of independent power supplies providing failure tolerance; a Solar Electric Propulsion Harness (SEPH) and Solar Electric Propulsion System Pipe-work (SEPP). In addition to the challenges brought about by operation at close proximity to the sun, this mission includes the first European operation of two ion thrusters simultaneously on orbit. Each PPU allows the operation of any one SEPT between the thrust range 40 – 145 mN, with simultaneous SEPT operation achieved using both PPUs. Thrust vectoring is achieved via a gimbal pointing mechanism.

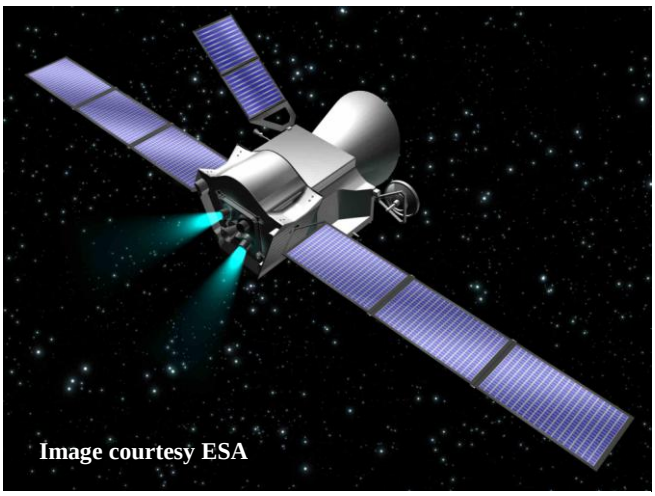

Figure 1 Bepi-Colombo composite

This paper describes the respective system architectures for the SEPS for BepiColombo, together with the qualification programmes underway. The approach to qualification of the SEPT is described, as developed through Assembly, Integration and Verification (AIV) activities leading up to the BepiColombo mission, including; mechanical integrity, Thermal Vacuum (TV), Electromagnetic Compatibility (EMC), Electromagnetic Interference (EMI) and thrust performance characterisation as well as the development of the necessary Ground Support Equipment (GSE) including Electrical GSE (EGSE), Mechanical GSE (MGSE) and Fluidic GSE (FGSE). Performance verification of a fully representative SEPS is considered to be an essential element in the qualification of the SEPT.

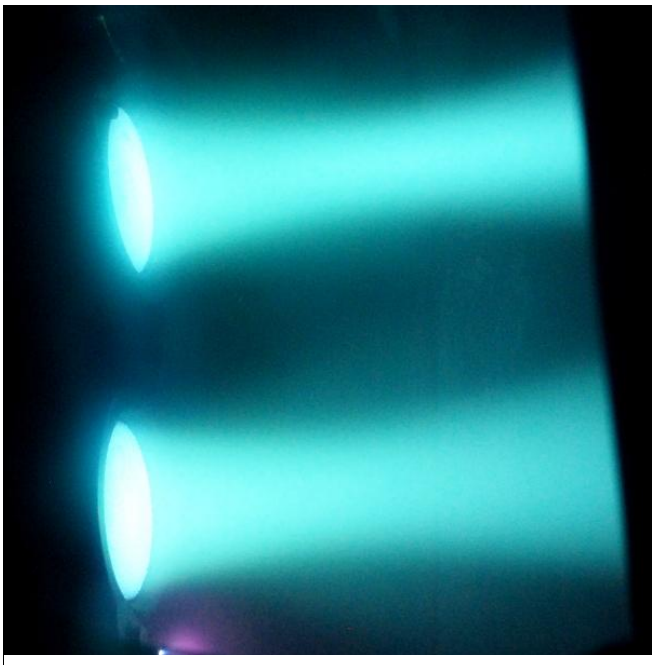

Figure 2 Dual ion thruster test conducted under the Technology Demonstration Activity

The SEPT (widely known as the QinetiQ T6) is a Kaufman configuration gridded ion thruster, first designed in 1995 to meet the needs of science and telecommunication missions in the 21st century. QinetiQ has completed a successful Technology Demonstration Activity (TDA) of a T6 thruster for risk reduction associated with Europe's first use of electric propulsion for a major science mission. These activities investigated new requirements such as sustained, stable operation over long thrust arcs, the simultaneous operation of two thrusters at high power in close proximity, low thrust interruption rates and the harsh thermal environment approaching the Sun. The T6 thrusters were designed using well established scaling laws developed during the design and development of the T5 thruster, which is currently flying on ESA's Gravity field and steady-state Ocean Circulation Explorer (GOCE) mission[2]. The SEPT has been further developed over the past 10-years to meet the requirements of both the BepiColombo and High Power Electric Propulsion System (HPEPS) programmes, an approach that maximises heritage transfer.

II. System Elements and SEPS Architecture

Critical to the SEPS system design is the redundancy and cross-strapping philosophy. The selected configuration of two PPUs with fully symmetric cross-strapping of T6 units to PPU outputs gains maximum benefit from the symmetry of the four engine configuration. This provides the most robust response to failure of any single unit. In particular, the ability to maintain equal distribution of total impulse between operational T6 units is maintained for any single unit failure in a BSM, DANS, FCU or a T6. This in turn minimizes the thruster life time requirement.

The resulting design provides for an elegant AIV sequence and plan. The number of units is minimized (only two PPUs without auxiliary electronic boxes), mounting and demounting units is straightforward with an integrated splice plate and the number of operating modes for testing and characterization is minimized. In addition, system mechanical and electrical symmetry means fewer operational patterns to verify in terms of thermal behavior.

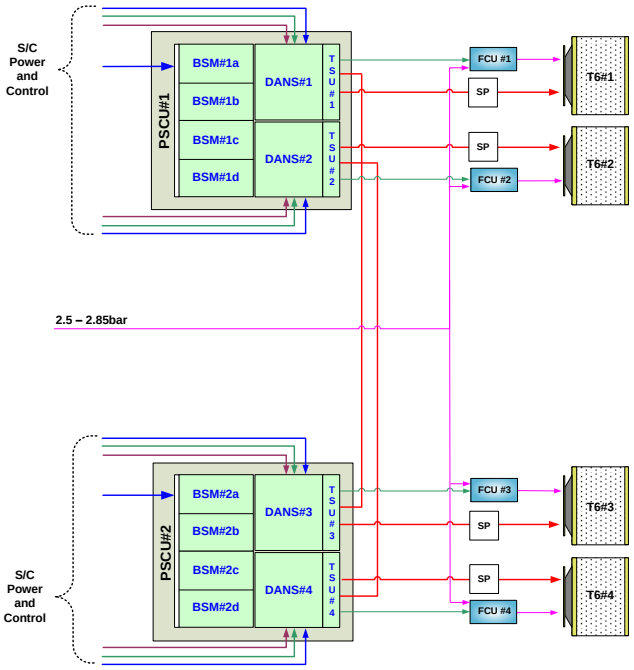

Figure 3 SEPS architecture providing guaranteed simultaneous thruster operation and impulse sharing

The system architecture is presented in Figure 3 and comprises:

- 4 x T6 thrusters
- 4 x Xenon Flow Control Unit (FCU) assemblies, each dedicated to a specific T6
- 2 x PSCUs, each with 4 beam supply modules and 2 DANS (discharge, accelerator grid and neutralizer supplies)
- 4 x Splice plates
- Harness and pipe work

A. Solar Electric Propulsion Thruster (SEPT) and Harness

The T6 thruster shown in Figure 4 is of conventional Kaufman configuration, with a DC discharge between a hollow cathode and a cylindrical anode where electron impact ionization provides a source of ionised propellant. The efficiency of this plasma production process is enhanced by the application of an electromagnetic field within the discharge chamber by an external solenoid set. A 22-cm grid system, forming the exit to the discharge chamber, extracts and accelerates the ions, to provide the required thrust. An external neutraliser cathode emits the electrons necessary to neutralise the extracted ion beam.

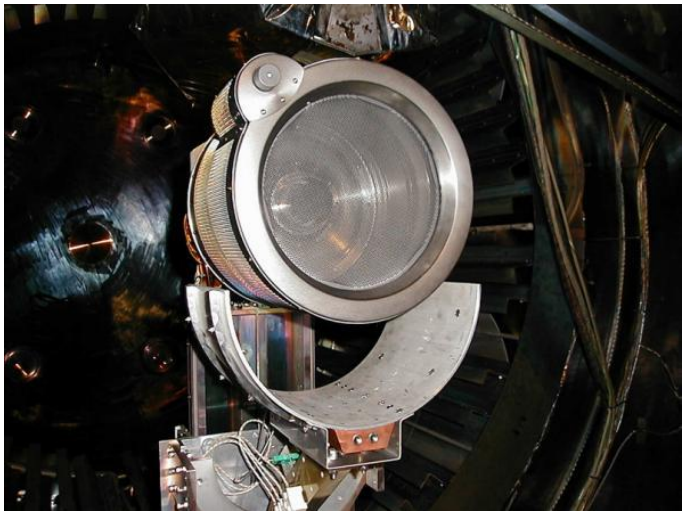

Figure 4 The photograph shows a T6 SEPT during preparation for the BepiColombo TDA tests to verify SEPT compatibility with Mercury thermal environment.

At an early stage of the programme it was recognized that the harness between the thruster and the power processing unit (PPU) was a critical system element and that it was

imperative that the system engineering of the harness must be performed concurrently with the thruster.

The design is driven by the high voltage, high current and high temperature operation in conjunction with the need to traverse the moving interface presented by the pointing mechanism. It was also recognized that to allow the mechanism and harness integration to be performed in isolation to the thruster (earlier thruster designs have always included an integral flying lead design) it was necessary to introduce a connector block on the thruster. To maximize heritage the harness design employs the same commercially available PTFE (corona free) coaxial high voltage cable technology qualified on the GOCE programme with the T5 ion thruster.

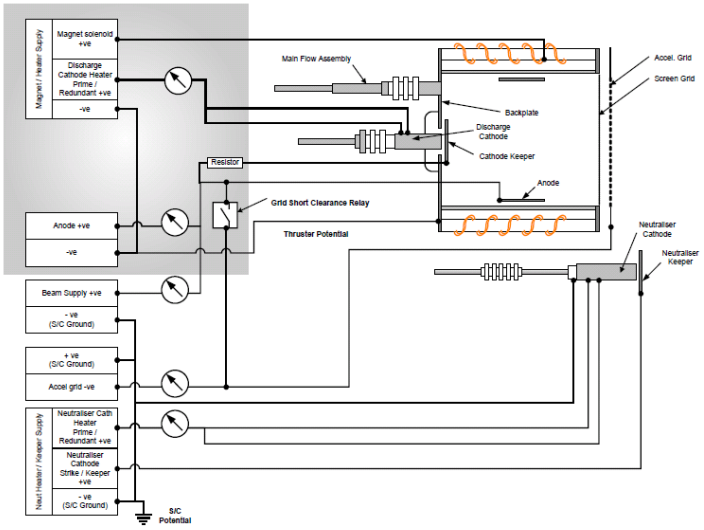

Figure 5 Thruster power supplies schematic

B. Power Processing Unit (PPU)

The Power Processing Unit (PPU) provides the required functionality to power and control the T6 thruster and the Flow Control Unit (FCU) as commanded by the satellite's on-board computer. The PPU also provides the necessary telemetry and telecommand interfaces to control and monitor all thruster functions. In order to minimize the mass and volume of the PPU its design takes advantage of the fact that a number of the thruster and FCU control functions can be supplied by a common power supply without impact to the performance or operation of the system. This results in a total of 5 power supplies being required to power the T6 Thruster as illustrated in Figure 5.

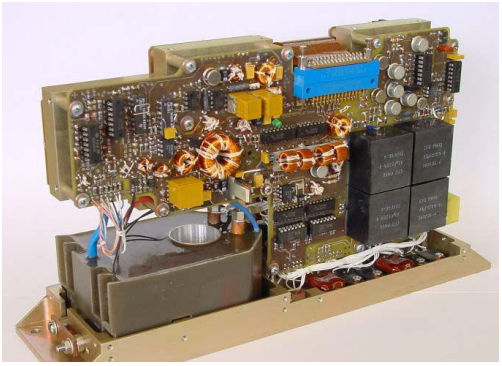

Figure 6 Assembled beam supply module

The five PPU thruster supplies are as follows: neutralizer heater (primary and redundant) and neutralizer keeper supply (the keeper can be powered by the same supply as the heater as the two are not required to operate simultaneously); accel grid supply, beam supply, anode and cathode keeper supply (the cathode keeper is operated in parallel with the anode supply), magnet and cathode heater (primary & redundant) supply (cathode heater and the solenoids share the same supply, as they are not required to operate simultaneously).

Where supply functions share a common transformer within the PPU, the changeover between supplies, is only performed when the supply is in a shutdown state, thus hot switching is eliminated. In addition to the above nominal functionality, the PPU design makes use of the high current capability of the Anode supply to provide a grid short burn-away function. This functionality means that should a conductive particle cause an electrical short between the Accel and Screen grids, which would cause the voltage

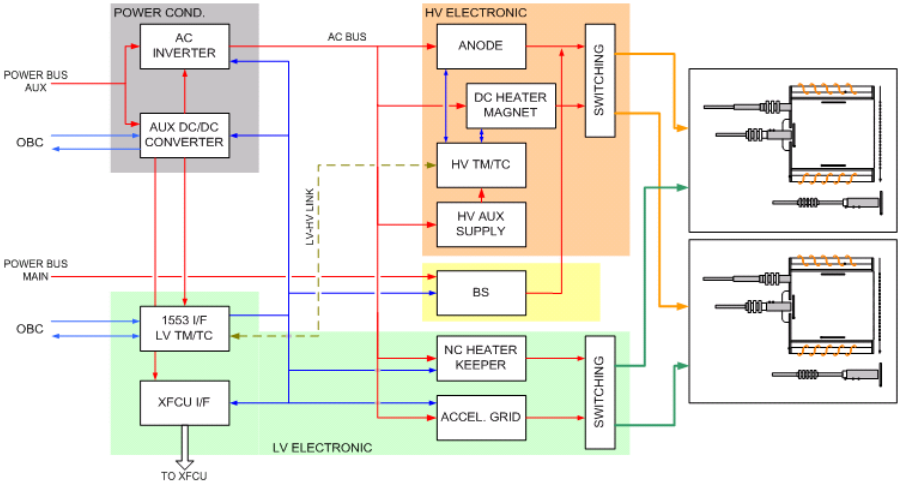

Figure 7 Schematic of PPU architecture

across the grids to collapse, and in the event that this particle does not 'self clear', the Anode supply can be switched to the Accel grid to 'burn-away' the contaminant.

The PPU design incorporates a Faraday housing as was employed in the IPCU for GOCE. In this design the high voltage referenced power supplies; i.e. the anode, solenoids, cathode keeper and cathode heater supplies, are enclosed in a housing which is floated at beam potential and the whole unit is isolated from the unit chassis via conventional ceramic isolation techniques. This concept has two major advantages. The first is that it virtually eliminates difficulties associated with parasitic elements within the high voltage (HV) referenced supplies, e.g. unexpected current paths for the common mode currents are contained within the enclosure. Secondly the power supplies can be readily designed without having to deal with any HV isolation design complexities, i.e. isolation is achieved once using simple ceramic stand-offs, because the components within the supplies are referenced to the HV enclosure. Each PSU is a single item in the T6 SEPS comprising two main functional elements; the beam supply and the DANS [2off]. The beam supply is comprised of up to 5 beam supply modules. In the case where 3 beam modules are required to fulfill the mission requirement a 4th beam supply module is also included. As such the beam supply is tolerant of a single Beam Supply Module failure, i.e. 4 for 3 parallel redundancies. There are 2 DANS assemblies within the PPU, providing 2 for 1 parallel redundancy. The outputs of each DANS are switched to either one of the north thrusters or one of the south thrusters. This enables the S/C thermal control to be simplified because the heat loads are always in the same place, i.e. provision does not need to be made for dissipation in two locations.

C. Flow Control Unit

During thruster operation the xenon flow control unit (FCU) , shown in Figure 8, will deliver propellant at the required mass flow rates to a single thruster. The FCU uses a proportional valve in closed loop control with a pressure transducer to control the pressure at the inlet to a fixed restrictor (at constant temperature). The pressure based control method is a simple and robust solution for the Main and Cathode flow control. It is a direct method of control based on the basic parameters determining the mass flow rate, i.e. pressure, temperature and the physical restriction.

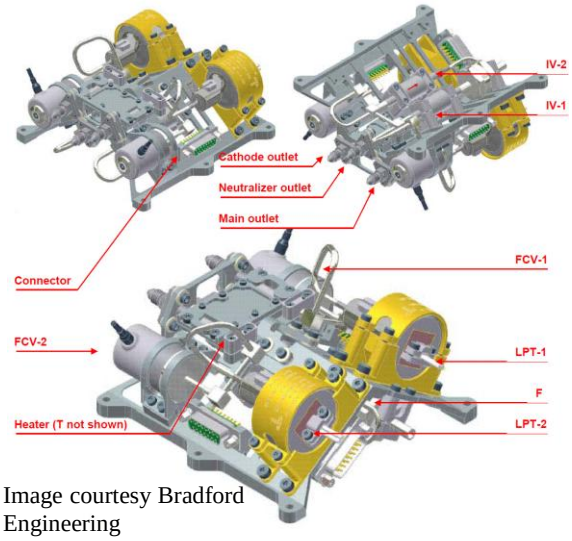

Image courtesy Bradford Engineering

Figure 8 FCU solid model

Pressure sensing is considered to be more dependable than mass flow sensing and less susceptible to temperature variations. It is preferable to minimize the variety of functional components and control methods in a single design. In this solution the Main Flow and Cathode feeds will use the same flow control components and method. The FCU includes a filter at its inlet to protect the system from particulate contamination. Immediately downstream of the inlet filter is a single mono-stable isolation valve as shown in Figure 9, after which the flow path divides into 3 parallel branches for the Neutralizer Feed, Cathode Feed and Main Flow Feed. The Main Flow Feed and Cathode Feed branches each contain a proportional flow control valve, pressure transducer and fixed restrictor. The Neutralizer Feed branch contains a mono-stable isolation valve and a fixed restrictor only. The Neutralizer Feed operates at a single fixed flow rate and can be operated independently of the Main Feed and Cathode Feed.

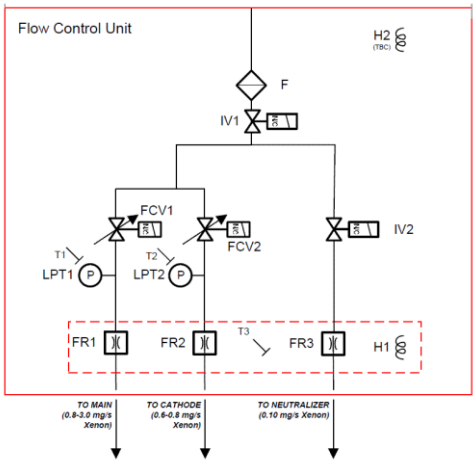

Figure 9 FCU schematic

Each valve type, IV or FCV, is capable of achieving the necessary internal leak tightness when closed, and both are normally closed devices so that in the event of a loss of power to those valves they would automatically close. Any combination of valves can be opened independently or simultaneously for test, venting and purging operations on ground or in orbit. The overall configuration of valves ensures that there are 2 in-series inhibits between the inlet

and each outlet, so that in the event that any one valve failing open or leaking excessively the propellant upstream of the XFCU can be isolated

III. SEPT Qualification Activities

Qualification tests formally demonstrate that the design, implementation, and manufacturing processes of the SEPT are fully compliant to specification requirements in environmental conditions harsher than nominal in order to provide a factor of safety and margin over the operational conditions. This verifies that the equipment complies with the requirements from its Technical Specification. The T6 thruster will undergo a stand alone qualification programme. The qualification test sequence to be performed using is presented in Figure 10.

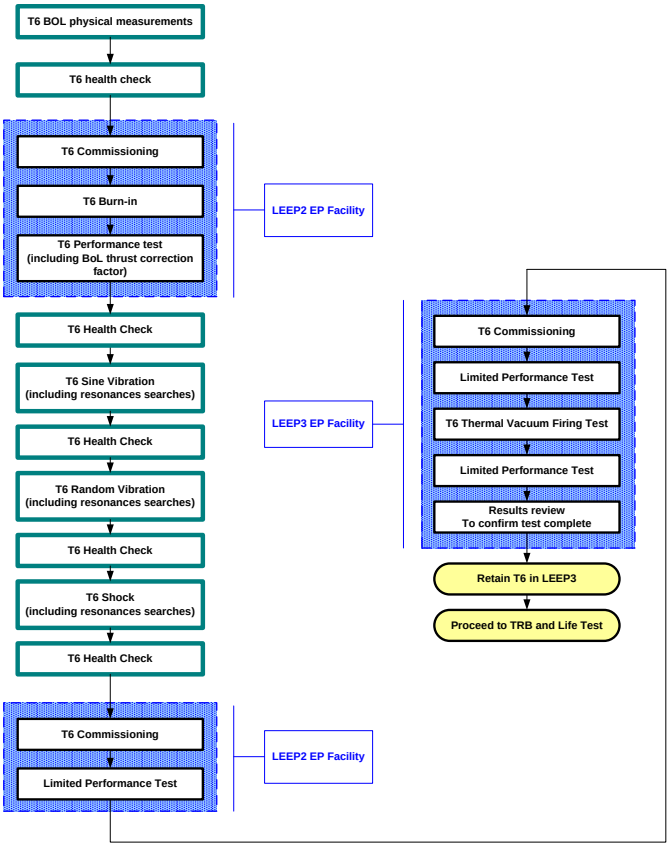

Figure 10 T6 unit level qualification test sequence

A. Qualification Approach

The SEPT qualification approach consists of a BoL performance characterization followed by an 8000 hour endurance test with periodic grid inspections followed by an EoL performance characterization and separate SEPS coupling test.

SEPT performance Characterization

A similar SEPT thrust characterisation approach has been adopted as that in the T5 (Artemis and GOCE) and T6 development (BepiColombo TDA, AlphaBus and Grid TRP) programmes, during which a number of different thrust balance concepts have been employed to provide a thrust correction factor (TCF). The TCF will then be subsequently applied to the electrical thrust level, calculated using the electrical parameters, to provide the actual thrust level. For the derivation of the SEPT thrust vector using a beam probe diagnostic, which is also specified for every SEPT firing test, it is necessary to accurately measure the alignment between the SEPT and Beam Probe Array (BPA). This is performed using a Digital Photogrammetric Alignment (DPA) technique to determine the thruster vector origin with respect to the beam probe array, typically with an accuracy <30µm.

8000-hour Endurance Test

The thruster will be subjected to an 8000 hr endurance test. Following each 2000 hrs the test will be suspended and the facility vented to allow a detailed inspection of the grid assembly. This will be achieved by removal of the grid assembly and inspection of the grids using a combination of white light interferometry (WLI) and a sub-micron coordinate measurement machine. In parallel with testing, the erosion of the grids will be modeled and correlated against the measurements obtained. Following the completion of 8000 hrs an end-of-life grid assembly will be manufactured, using the modeling predictions for end-of-life and fitted to the thruster. The end-of-life performance will then be verified.

SEPS Coupled Test

An important aspect of the BepiColombo SEPS system verification will be performed at a full SEPS system level, incorporating all of the flight components. MGSE will be produced that will allow the Thrusters, PPUs, XFCUs and pipe-work/harness to be integrated in a fully flight representative manner. During this test campaign all of the possible/applicable thruster and PPU/FCU combinations will be verified including thrust vector measurement during simultaneous thruster operations.

B. Beginning of Life Thrust Correction Factor

The thrust correction factor is derived at the BoL from direct thrust measurements. The velocity of the ejected ions depends only on the beam potential and the Neutraliser Coupling Potential (NCP), whereas the thrust is a function of velocity and the ion beam current. At different thrust levels the divergence of the ion beam changes and therefore the resultant cosine losses also vary. The variation of the beam divergence is in turn dependent on the plasma density in the thruster discharge chambers prevalent at the different thrust levels and the grid spacing. Both of these factors are consistent between thrusters of the same build standard. The TCF is therefore dependent on the presence of doubly charged ions in the beam; the thrust contribution of neutral propellant atoms; variations in the NCP across the thrust range and thrust vector misalignment with the thruster geometric axis. The TCF is defined as being the ratio of actual thrust (based on a direct balance measurement) to electrical thrust (based on electrical parameters). The thrust balance is mounted to the same structural ring as the beam probe arm and is shown in Figure 11.

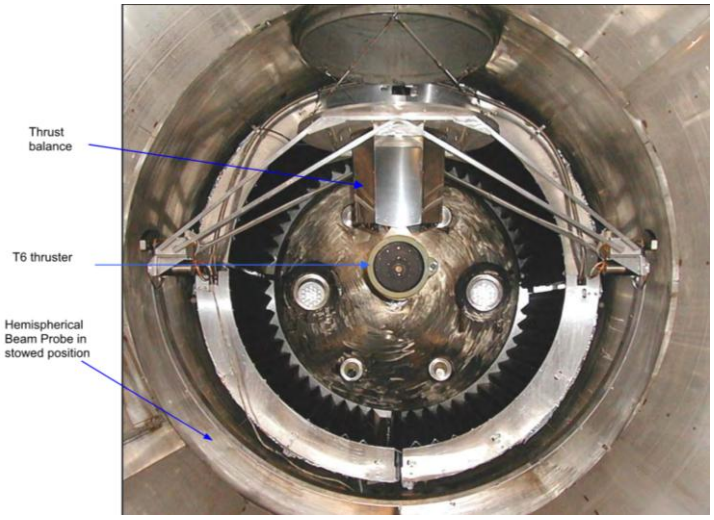

Figure 11 Photographs showing the Ion Beam Probe Array within the 3.8m LEEP 2 chamber

Thrust Balance

The balance, shown in Figure 12, consists of a swinging parallelogram pendulum design and contains solenoid/magnet force actuators as a method to produce an equal and opposite force to hold the thrust balance in a null position. To overcome the inherent problem of null-point drift due to residual thermal and mechanical drift, and low frequency vibration, a second, identical pendulum balance (with a dummy mass to represent the thruster) and control system is included. Its output gives a direct measure of the low-frequency noise and null-point drift, which is used to interpret the drift of the primary balance such that it can be accounted for to give the balance response relative only to the thrust force applied by the SEPT. In order to minimise the potential for thermal drift, the thrust balance is primarily manufactured from Invar with a low thermal expansion coefficient.

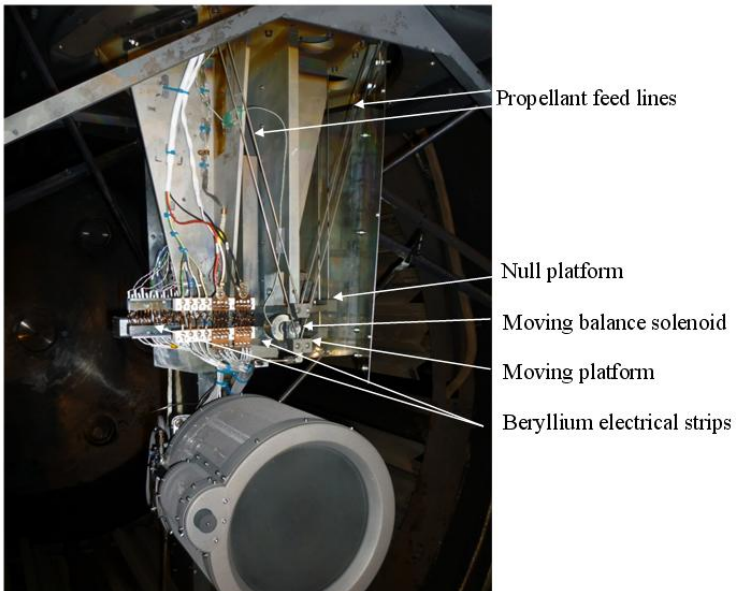

Figure 12 Photograph of the EQM SEPT mounted to the thruster back plate. The protective covers normally fitted to the thrust balance have been removed to show the construction of the balance system.

A displacement transducer (Renishaw grating encoder 0.1µm resolution) with a 19.66MHz decoder/interpolator detects the movement of the thrust balance caused by the application of a thrust force. A controller with a tuned frequency response accuracy applies an equal and opposite force to restore the null position of both the thrust and null balance. The platforms contains three solenoid/magnet pairs; one pair mounted to the moving balance to restore the null position thrust balance, a second pair mounted to the thrust balance for thrust balance calibration, and a third pair mounted to the null balance, again to restore the null position.

The solenoid current electronics converts an input voltage from the decoder into an output current. This output current is passed though the solenoid to generate the driving force on the magnet. The voltage input to the current source is also provided as the final output of the thrust balance. The thruster is weighed prior to integration onto the thruster back plate and appropriate counterweights are added to the null balance such that both the null balance and thrust balance are of equal weight to give an equal response to external vibration in order that the compensation is reasonable.

In order to feed electrical and fluidic lines to the thruster, the connections must traverse to the moving platform of the balance. Any physical connection to the moving balance introduces a form of spring constant. Fluidic connections and high current electrical connections display current or flow rate dependant heat flux which induces changes to their mechanical properties. These responses are extremely difficult to fully characterize, hence all electrical connections to the moving balance are made by thin beryllium jumpers in back to back pairs as shown in Figure 13. This arrangement presents a consistent and very low spring constant. The problem of routing fluidic connections to the thruster is mitigated by suspending the thrust balance platform from the fluidic lines, thus the lines are unable to produce significant moments on the balance through the thrust axis. Prior to the start of the EQM test campaign, a thermal control and monitoring system was installed on the moving balance, null balance and supporting structure. During testing, PID controllers in the heating circuit maintain the solenoids at a constant 60°C.

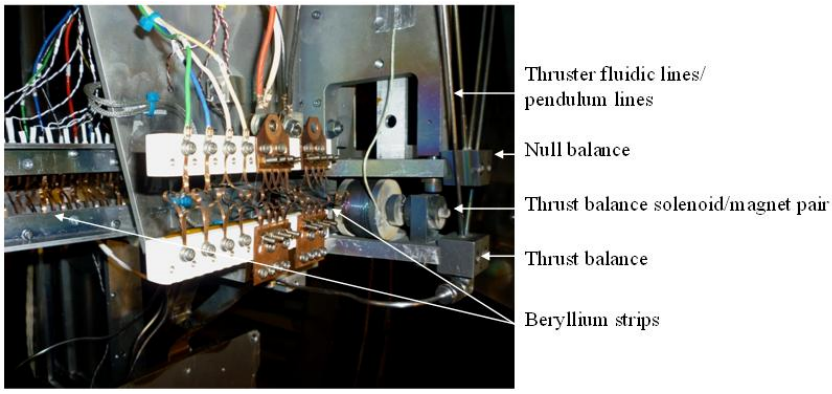

Figure 13 Electrical and fluidic connections

Thrust Balance Calibrator

At the rear of the thrust balance an in-situ calibration system is fitted to the supporting structure. The system provides a means to conduct calibrations under vacuum conditions immediately before, after or during thruster firings. The calibrator allows a series of weights to be sequentially suspended from a connecting line to the thrust balance platform. A low friction pulley allows the line to turn through 90° and connect perpendicularly onto the thruster back plate. The pulley bearing consists of a low friction needle point bearing to minimize hysteresis.

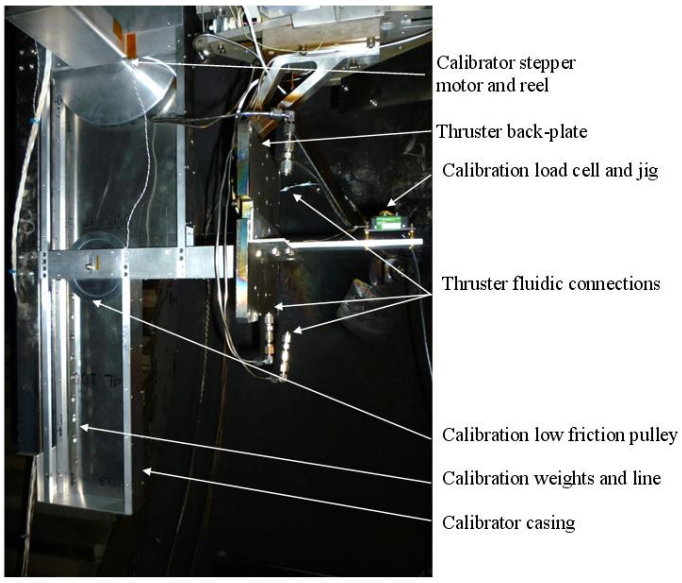

Figure 14 Thrust balance calibrator and load cell

By knowing the exact force applied by the weights to the balance and characterizing this force against the thrust balance response, which acts to maintain the null position, a calibration curve (Volts/mN) can be generated. The calibration curve can then be used to quantify the response of the balance during thruster firings. The calibration weights are shown in the highest applied force condition, with all of the weights acting on the balance. As the stepper motor and reel rotate, weights discreetly transfer from the line tensioned to the thrust balance to the line hanging from the reel. The calibrator stepper motor is controlled via Labview software in which preset calibration profiles can be run, including stepper motor position and residence time at the calibration point.

An accurate characterisation of the in-situ calibration weights themselves was made by mounting a load cell to the thruster back plate via a jig and attaching the weighted line directly to the transducer. Weights were sequentially added and removed to give a detailed data set from which to characterise the force applied by the

calibrator and quantify associated error and repeatability. Refinement of the calibrator resulted in repeatability better than 92.6μN at any weight setting over 12 repeat checks of the 8 weight settings (0-160mN) for the final calibration of the weights prior to EQM thruster commissioning.

Thrust Measurement Method

The balance assembly is exposed to the most significant thermal flux during thruster operation. Since the thruster is required to reach thermal equilibrium, taking some hours, before a thrust measurement is made, this period leaves open the possibility of zero drift. Assuming an in-situ calibration is made before thruster start-up, although the null balance can be used to characterise drift throughout this period, however this leaves no opportunity to make a 'zero point' check whilst the thruster is operating. Therefore in order to absolutely minimise the potential for drift by using 'zero point' checks, thrust measurements are made by switching off the thruster and propellant flows after thermal equilibrium is attained, prior to making a calibration. This gives the opportunity to make a zero check immediately after switch-off taking the delta thrust balance response, followed by 6 calibrations with 3 intermittent zero point checks. The zero checks can therefore be used to correct for any small deviations in the drift of the null balance and thrust balance. This leaves minimal error associated with a long term drift between the thrust measurement and respective calibration. An ascending followed by descending calibration profile also maximises any hysteresis in measurements giving a worst case error value.

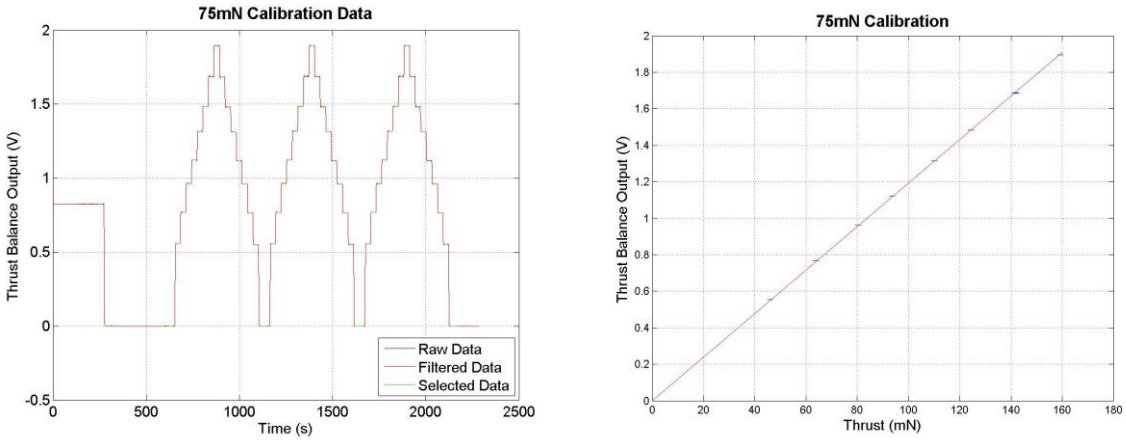

Figure 15 Typical thrust measurement delta followed by thruster switch-off (left) and the resulting calibration analysis showing error bars (right).

A typical thrust measurement and calibration profile is shown in Figure 15. A Matlab program was developed to automatically extract information from the data, for repeatability, speed and to eliminate any human error component in the analysis. The program corrects for zero drift and locates the initial thruster switch-off point and selects a portion of the data one minute before and one minute after switch-off. The program then analyses a 70% centre section of the data, representing a 42 second period at 100Hz, giving a mean value with associated standard deviation. This 'cropping' is done so as not to include any transitional data at the edges of the steady state values in the mean value. The program repeats this method to attain the calibration data for each calibration weight setting.

Sources of systemic or random errors introduced throughout this process are analyzed in detail flowing down from the national measurement standard. An overview of the measurement process and uncertainty analysis is shown in Figure 16. Typical repeatability of the thrust measurement is better than 0.2mN with a standard error of better than ±0.4mN

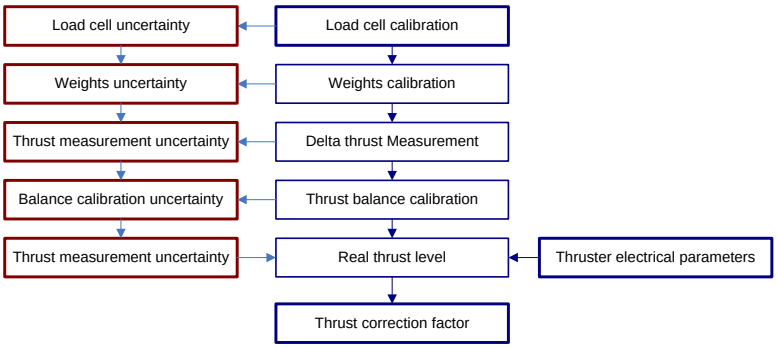

Figure 16Measurement methodology (blue) and sources of systematic error (red)

Primary sources of noise in the thrust measurement are shown to be at 5.5Hz and 6Hz with harmonics extending into the tens of Hz as shown in Figure 17. Primary sources of noise are cryopumps/ cryoheads and compressors.

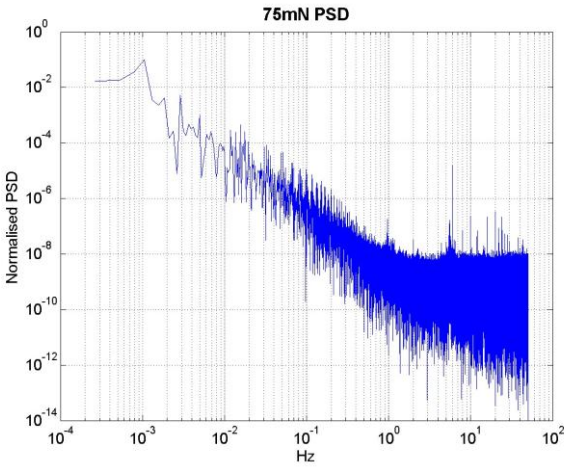

Figure 17 Power spectral density (75mN)

Thrust Vector/Beam Divergence Analysis

Thrust generated by a gridded ion thruster is a result of the net force acting on both the screen and accelerator grids. The *Thrust Vector* defines the magnitude and direction of the thrust and can be determined from the centroid of the beam current distribution measured downstream of the thruster. Erosion and movements of the grids cause the thrust vector to vary over time; beam measurements during thruster lifetime tests enable the expected variation and stability of the thrust vector to be evaluated.

The LEEP2 and LEEP3 facilities at QinetiQ each house a beam probe diagnostic system comprising a 2.4m diameter semicircular, rotatable arm to which 11 screened faraday cup probes are mounted. The faraday cup probes are spaced equidistantly along the centre section of the arm and are aligned by laser to point to the centre of the accelerator grid of the thruster mounted in the chamber. The beam probe arm is driven by a stepper motor and rotated about its axis in order to measure ion beam current density over a 2D hemispherical surface, with the thruster located at the origin of the sphere.

The relative alignment between the beam probe system and thruster is accurately measured by use of Digital Photogrammetric Analysis (DPA). In this process, multiple images are taken of specially coded targets mounted to the beam probes, beam probe arm and to an alignment device mounted to the thruster, with a calibrated digital SLR camera. Four DPA targets mounted to the thruster alignment device enable a local reference frame to be defined, known as the 'Alignment Cube Axes' (ACA) indicated in ***Figure 18***, which permits the measured positions of the faraday cup beam probes to be linked to known points on the thruster body.

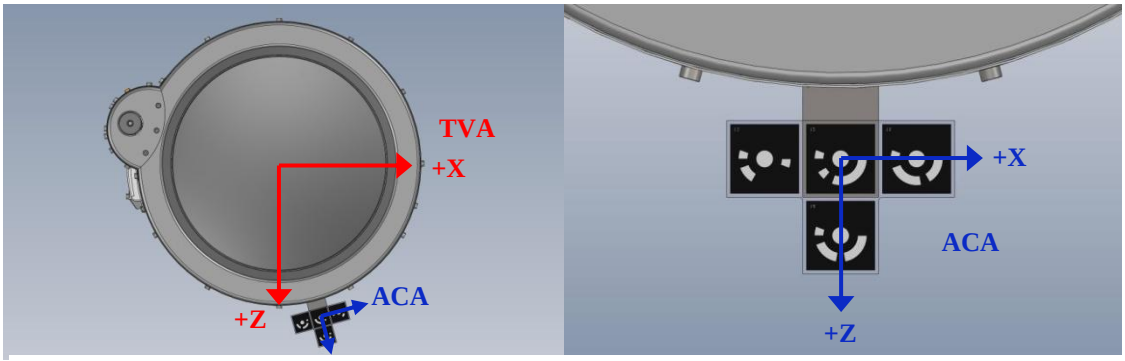

Figure 18 Drawings of the DPA alignment device mounted to the T6 thruster displaying the orientation of the Alignment Cube Axes and Thrust Vector Axes.

The images are processed by the DPA software package 'AICON 3D Studio', which is able to triangulate the positions of the DPA targets in the images given a known reference distance, provided by two calibrated scale bars manufactured from carbon fiber and positioned between the thruster and beam probe system (as shown in Figure 19). A calibrated cross-bar is also provided to define a reference frame for the images. Image acquisition and analysis can be performed within a period of 10mins for a typical set-up, providing a rapid and highly accurate method of alignment measurement.

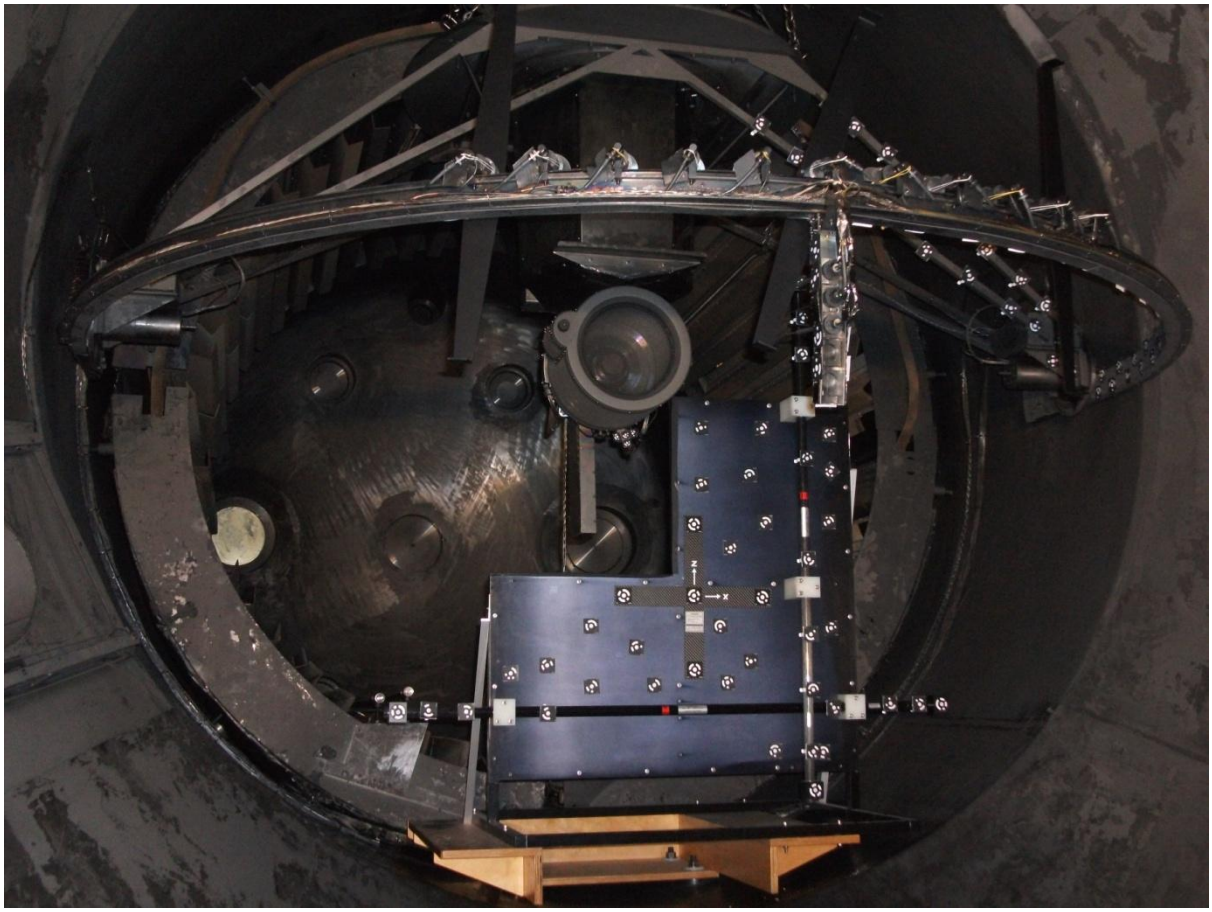

Figure 19 Image of the T6 EQM thruster mounted within the LEEP2 vacuum facility with beam probe system and DPA alignment devices.

The positions of the DPA targets on the alignment device with respect to physical points on the thruster body are measured by a Coordinate Measuring Machine (CMM) located in-house at QinetiQ. The CMM measurements also permit a measurable coordinate system to be defined for the thruster for use in mechanical inspection and verification activities, the geometrical centreline of the thruster to be measured and the centre of the Accel grid to be measured. The origin of the thrust vector, representing the center of impulse at the grids, is taken to be the centre of the Accel grid; a reference frame is therefore also defined at this point, termed the 'Thrust Vector Axes' (TVA) (indicated in Figure 18).

The coordinates of physical points on the thruster determined by CMM are combined with the coordinates of the beam probe system and alignment device determined by DPA using the 3D metrology software package 'Metrolog XG'. A set of transformation matrices determined from this combined set of measurements enables the thrust vector, identified from the maximum of the 2D spatial profile of beam current density measured by the beam probes, to be given with respect to the Thrust Vector Axes. The direction of the thrust vector can be given as a horizontal (α) and vertical angle (φ) with respect to the thrust vector axes, as depicted in Figure 20.

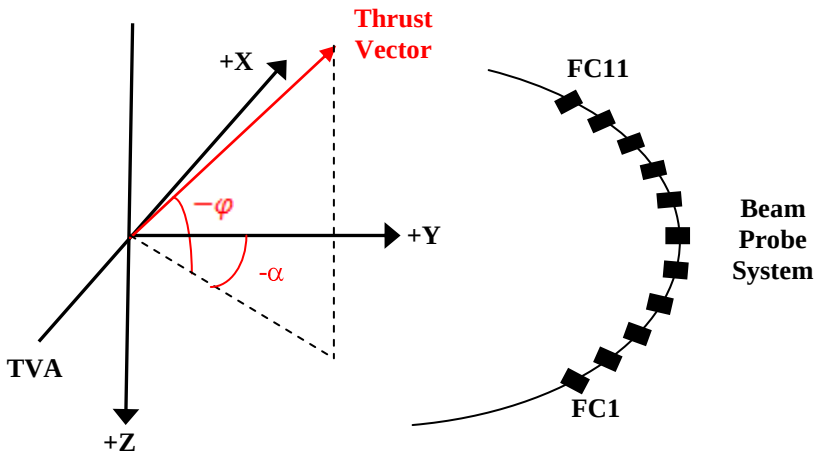

Figure 20 Diagram indicating the horizontal (α) and vertical angle (φ) components of the thrust vector with respect to the Thrust Vector Axes (the horizontal angle is negative with respect to the +X-axis and the vertical angle is negative with respect to the +Z-axis

A 2D integration is also performed on the measured beam current density to determine a value for the total measured beam current (I_b). Beam divergence (*defined as the half-cone angle that incorporates 95% of the total beam ions*) can therefore also be determined from the beam probe measurements by iterating to find the angle which includes 95% of the total measured beam current:

$$0.95\ I_b = \sum_{\theta=0^\circ}^{\theta=\beta} I_\theta$$

The thrust vector and beam divergence were measured during initial performance characterization of the T6 EQM SEPT at four nominal thrust levels of 75mN, 100mN, 125mN and 145mN. Three beam probe sweeps were performed for each thrust level; Table 1 and Table 2 present the results of the thrust vector and beam divergence.

Thrust Level (mN)	Beam Divergence (°)
75mN	23.491
100mN	22.107
125mN	20.101
145mN	18.048

Table 2 Beam divergence measured at T6 EQM thrust levels

Thrust Level (mN)	Value	Thrust Vector (TVA)	
		Horizontal α(°)	Vertical φ(°)
75mN	**Mean**	**-0.1470**	**-0.4279**
	deviation (1σ)	0.0108	0.0192
100mN	**Mean**	**-0.2427**	**-0.4892**
	deviation (1σ)	0.0098	0.0136
125mN	**Mean**	**-0.2594**	**-0.4640**
	deviation (1σ)	0.0111	0.0239
145mN	**Mean**	**-0.2689**	**-0.4579**
	deviation (1σ)	0.0080	0.0167

Table 1 Thrust vector determined with respect to the Thrust Vector Axes for the T6 EQM thruster

2D and 3D plots of beam current density for a typical beam probe sweep are given in Figure 21 and Figure 22, providing an indication of the thrust vector and beam divergence.

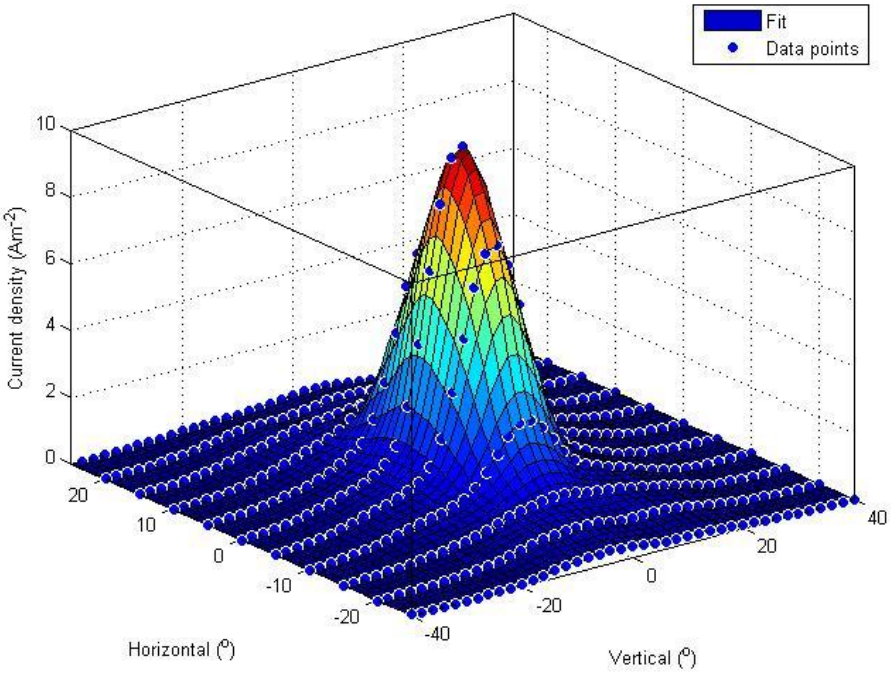

Figure 21 3D plot of beam current density measured for the T6 EQM thruster at 75mN.

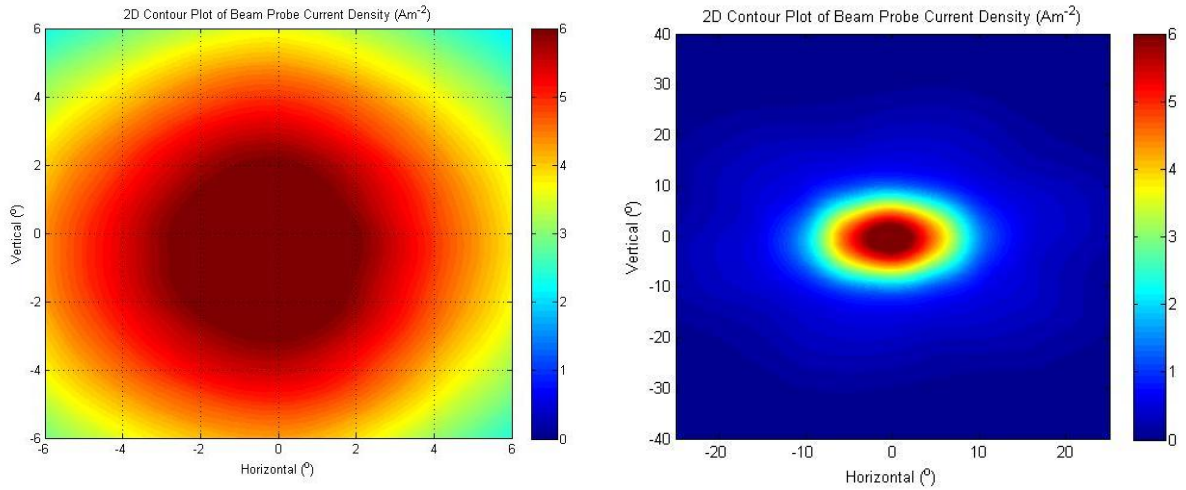

Figure 22 2D plots of beam current density measured for the T6 EQM thruster at 75mN.

C. Grid Lifetime Verification via Modeling Predictions and Measurement Validation

A grid lifetime modeling approach that has been employed on the BepiColombo SEPT, is referred to as the alternative life test approach. The extrapolation of the Accel grid erosion to the conditions anticipated following operation at 145 mN for a period of 26,000 hrs (26,000 hrs is the anticipated qualification requirement for the SEPT and therefore represents a factor of 1.5 times the flight requirement) are to be modeled. To provide additional margin the analysis presented in this section assumes that the full 26,000 hrs operation is performed at 145 mN; i.e. 13MNs.

The initial stage in the lifetime verification of the SEPT, prior to any performance characterization or endurance testing, is to assess the compatibility of the SEPT grid system with the BepiColombo qualification requirements. This assessment has been performed previously using TDA/TRP data, with a number of basic assumptions with regards to the rate of Accel grid bore erosion.

There are limitations to the data and techniques that have been previously employed, in that the extrapolation of the grid erosion assumes a linear evolution. In the case of the Accel grid this means that the volume loss rate remains constant with time. This limitation will be addressed by employing a validated ion optics code (or a suite of codes) to progressively analyze the grid optics in their various eroded conditions periodically throughout the endurance test. This will highlight any trends that may differ from the linear assumption. This is not immediately possible however because the existing ion optics modeling code (SAPPHIRE) is a 2D code and has to assume symmetry about each aperture. This approach is perfectly valid for the Accel grid aperture bore erosion however the Accel grid downstream face erosion phenomena are clearly non symmetric and cannot therefore be simply analyzed. These erosion mechanisms will require the use of a 3D ion optics code.

To address the limitations described in the section above, it is planned to adapt an existing COTS 3D ion PIC code (KOBRA) and employ it for the modeling of the grid erosion mechanisms currently not possible with the 2D SAPPHIRE code. During the 8000 hour endurance test of the EQM T6 it will therefore be necessary to take measurements at key intervals (at 2000 hour intervals) to measure the erosion rates of the Screen and Accel grids in order to validate predictions of the ion optics model. The ion optics model and experimental erosion data will then be used to verify the compatibility of the EQM grid-set with the BepiColombo requirements. Following measurements of the EQM grid-set at key stages of the 8000 hour endurance test, the eroded configurations and resultant grid spacing's are identified. The ion optics code will then be used to assess whether or not the grids can be operated at the demanded beam current without inducing electron back-streaming for an EoL condition. In the following sections, the erosion mechanisms and the techniques employed to measure grid erosion to a very high accuracy are discussed.

Accel grid erosion

The Accel grid (a photograph of which is presented in Figure 23) is fabricated from high purity, high density amorphous graphite and is manufactured using standard computer numerically controlled (CNC) machining techniques, including the drilling of the ~7300 apertures. The grid is mounted to the front pole via flexible supports and sputter shielded alumina insulators.

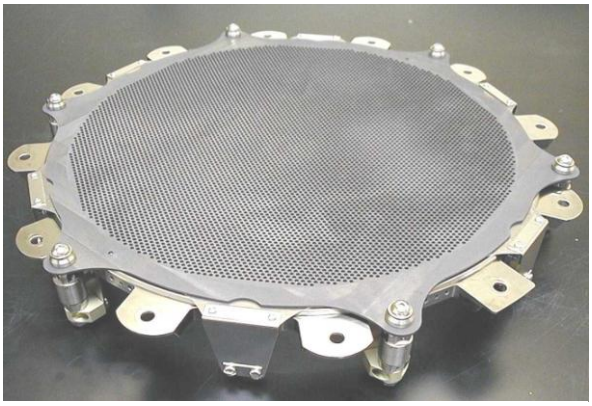

Figure 23 Photograph showing Accel Grid mounted to the Grid Assembly

Accel grid erosion occurs due to sputtering of the grid by xenon ions. In the case of the Accel grid there are two processes of sputtering by Xenon ions, these are:

- direct impingement of primary beam ions
- impingement of charge exchange ions

Direct impingement occurs when the ion beamlet exiting through a set of grid apertures (i.e. screen grid then accelerator grid) is either too large or defocused such that the ions strike the downstream region of the Accel grid apertures. Direct impingement however is only experienced at the extremes of the available thrust envelope and through ion optics simulations the T6 grids have been designed to eliminate this effect. As such this mechanism is eliminated.

Charge exchange (CEX), resulting in the creation of a slow moving ion and a fast neutral, are created by the interaction of the ion beam with neutrals exiting the thruster or interaction of the ion beam with background facility gas, either at the grids or downstream of the thruster. The original high energy beam ion continues on the same trajectory but as a fast neutral. The newly created CEX ion however does not posses the linear momentum imparted by the field between the grids; its trajectory is governed by the electric field at the point where it was produced. The CEX ions are therefore accelerated towards the negatively biased Accel grid, which then bombard the surface causing sputter erosion on impact. 2D modeling predictions from the existing Sapphire code are shown in Figure 24.

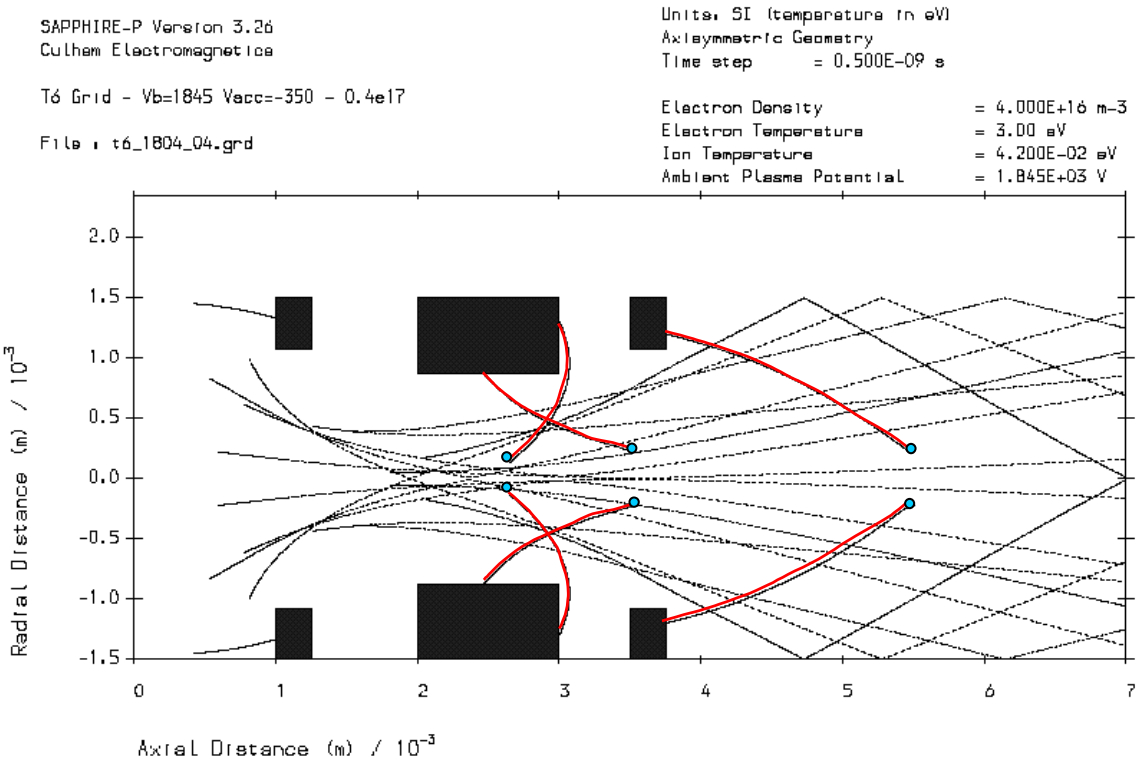

Figure 24 Ion optics modelling indicating the trajectories of charge exchange ions Note the points at which the CEX ions are created indicated as BLUE dots. Their subsequent trajectories are indicated as RED lines

Charge exchange erosion of the Accel grid cannot be eliminated and occurs at all thrust levels. It can however be minimized by controlling the neutral propellant number density. During operation in space these neutrals can only come from the thruster and Neutralizer. To this end the propellant utilization efficiency of the discharge chamber, defined as the fraction of propellant usefully employed in the ion beam divided by the total propellant flowed in to the discharge chamber, is maintained at as high a level as possible. This minimizes the CEX ion production rate, and therefore, Accel grid erosion rate whilst also maximizing the thruster ISP.

During ground testing there is an additional population of neutrals which originate from the facility background pressure; i.e. the vacuum facility has a limited pumping speed and therefore propellant injected into the facility by the thruster are not all removed immediately. There is therefore a considerable difference between operation of an ion thruster in space during flight and operation in a facility during qualification. The CEX ion production from the thruster alone is a lot less than that produced when interacting with the facility. To ensure that facility CEX is minimized as best as possible, chamber pressures less than 1 x 10-5 mbar (0.001 Pa) is necessary. These additional impacts on grid erosion effectively mean that the ion optics must be designed for qualification in a ground test facility.

Pits and Grooves and Aperture Erosion Pattern

This type of erosion is most prominent in two grid systems in which a large fraction of the CEX ions impact the downstream face of the Accel grid. This occurs by CEX ions streaming back toward the thruster from the charge exchange plasma produced downstream by interactions between the facility background neutrals and the ion beam. The CEX ions are repelled by the beamlets and are therefore effectively channelled into regions of lessening charge density, which are situated between the beamlets. In particular, points between any three beamlets have less charge than regions between any two. The CEX ions are therefore accelerated towards the exposed grid web and strike it at high energies.

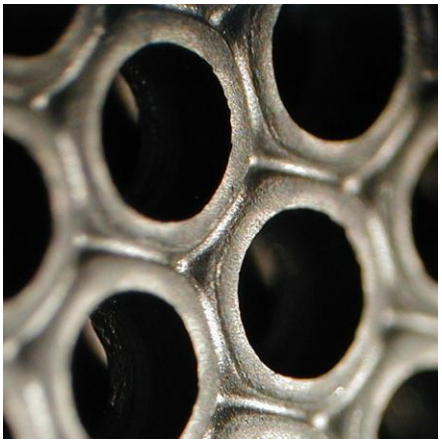

Figure 25 Pits and grooves erosion on Accel grid

The resulting erosion pattern complements the geometric configuration of apertures creating hexagonal erosion patterns as

shown in Figure 25. Common terminology for the erosion characteristics is 'pits' and 'grooves', pits being the deeper erosion regions and grooves the shallower erosion regions.

At the same time as the pits and grooves are developing, CEX ions erode the apertures. This results in an increase in the open area of the downstream face of the grid as shown in Figure 27. More erosion occurs at the downstream face than on the upstream, resulting in conical or chamfered grid apertures. This type of erosion is the key limiting factor in Accel grid lifetime, as the EOL condition (i.e. the onset of electron back streaming) is made more likely with apertures with larger diameter and thinner cross section.

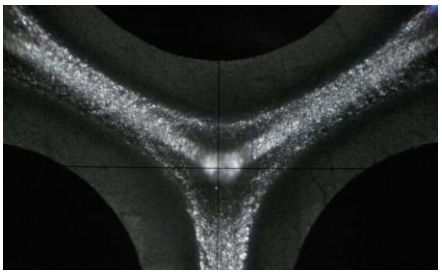

Figure 26 Views of of Accel Grid Pits and Grooves erosion present in twin grid configurations

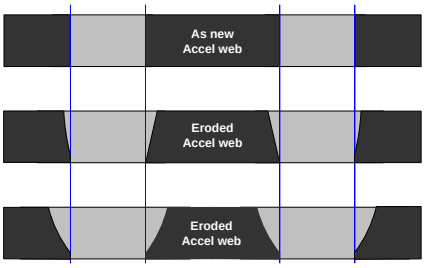

Figure 27 Schematic showing the shape evolution of 2 Accel grid apertures

Initial Accelerator Grid Erosion and Alignment Measurements

During the 8000-hour endurance test, these Accel Grid erosion mechanisms are required to be measured using the 3-Axis coordinate measurement machine (CMM) located at QinetiQ Farnborough, that will show the evolution of the Accel grid bore. The technique employed is a 3-axis coordinate measurement machine (CMM) which senses contact with the grid surface using a ruby tipped stylus. The contact approach eliminates any operator errors associated with optically identifying the edge. At each measurement stage the objective is to determine the profile of each aperture, by measuring the diameter at different distances from the downstream surface of the grid, as illustrated in Figure 29.

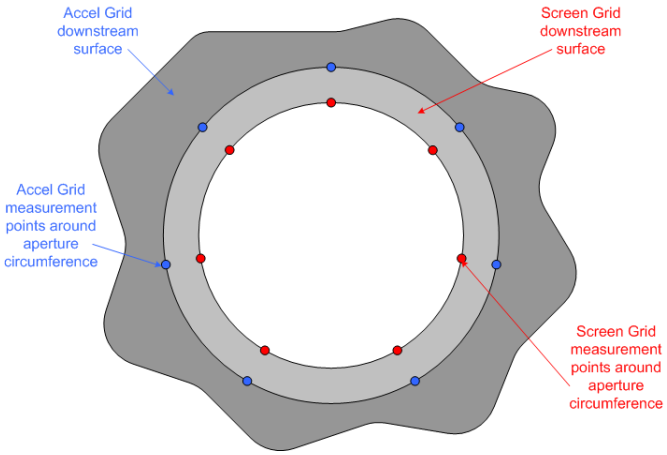

Figure 29 Accel to Screen Grid In-Situ Alignment measurement points

Figure 28 CMM located in the Y72 clean room laboratory

The CMM located in the Y72 laboratory at QinetiQ (Figure 28) is a 3-4 micron device, however it is important to note that this accuracy applies across the full operating volume of the machine (600mm x 800mm). If limited to a volume commensurate with each Accel grid aperture however the accuracy is dramatically better and following an assessment of the machine and test measurements a repeatability of ±1µm has been demonstrated.

The diameter and centre of the aperture is assessed by measuring points around the circumference and then calculating the best fit circle to these points. This is performed at multiple points down the bore. In addition to the measurement of the Accel Grid, the T6 grid assembly has been purposely manufactured with four holes on the screen grid smaller than the holes on the Accel grid so that in-situ alignment measurements (without removal of the grid-set) can be made. In addition to the aperture measurements, the CMM was also used to measure the 'pits and groove' erosion on the downstream face. This was achieved by moving the CMM stylus across the webs taking surface measurements at 0.1mm increments between apertures in both the X and Y axes.

Grid Evolution Measurements during Endurance Testing

At the beginning of life, every new Accel grid experiences an initial 'burn-in' phase during which the Accel grid aperture bore erosion is higher than normal. Prior to the 8000 hr endurance tests the EQM thruster will undergo a series of commissioning, qualification and Thrust Correction Factor determination tests. These tests will only constitute a few hundred hours of operation; however, this is deemed a sufficient length of time for burn-in to occur. It is therefore essential to conduct erosion measurements on this grid-set after these tests and before the start of the 8000 hr endurance test to establish a baseline and allow a meaningful, reliable trend to emerge in subsequent measurements.

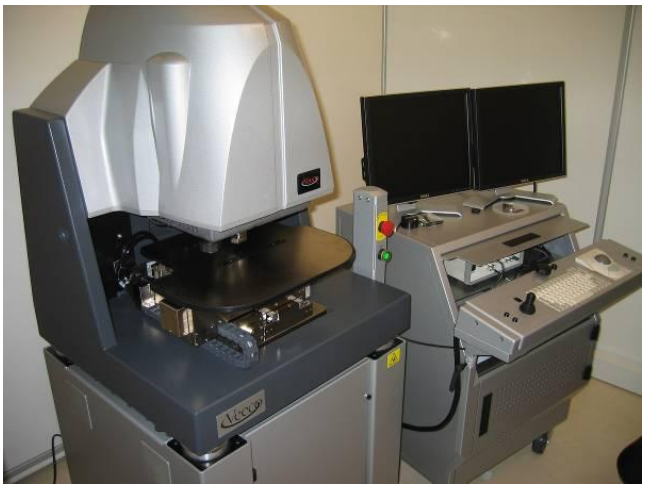

Figure 30 Photograph of the Veeco NT3300D White-Light Micro-Interferometer

At each 2000 hr test interruption the thruster will be subjected to electrical health checks prior to and following vacuum facility venting. After venting, the grid assembly will be removed from the thruster and transported to QinetiQ in the UK for measurement. Initially the grid set will be photographed in detail to record the visual condition of both grids and will then be subjected to a series of measurements using the white light interferometry (WLI) at QinetiQ Malvern, shown in Figure 30. It is not intended to dismantle the grid assembly because of concerns with re-alignment; i.e. any changes in the alignment of the grids will result in a thrust vector change and could potentially mask natural long term thrust vector migration trends. It is therefore not possible to employ the WLI to infer the Screen grid thickness as was the case during previous measurement techniques (i.e. with a stand-alone Screen Grid). In the case of the Accel grid the WLI will be used to characterize the downstream surface of the Accel grid; i.e. the 'pit' and 'groove' erosion.

The principle capabilities of the instrument are listed below:

- Z Range: 1 mm
- Z Resolution: 1 Å
- XY Range: 100 mm
- XY Resolution: 1 – 2 µm

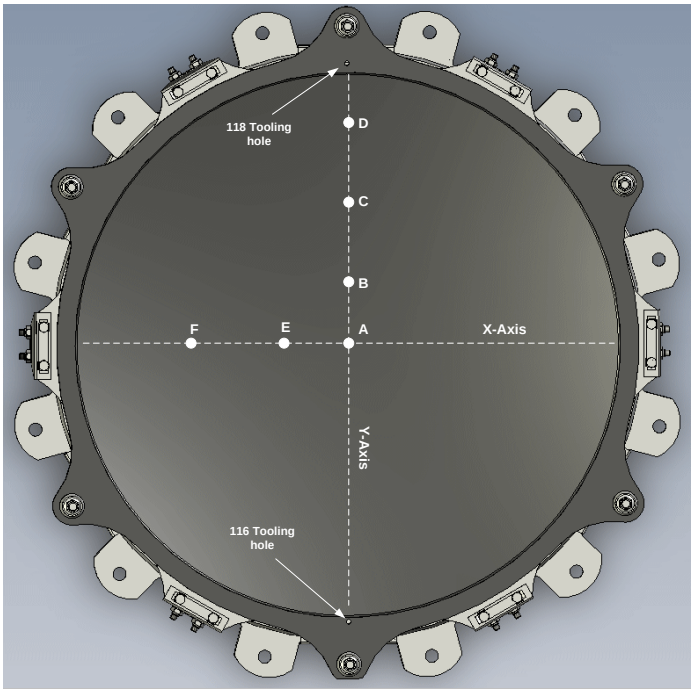

Figure 31 X-ray and WLI measurement locations on the T6 grid assembly

The Screen grid thickness will be determined using an X-ray absorption technique, and this information in turn will be used as a validation tool of the ion optics model (mentioned previously). Following a targeted development programme it has been determined that reliable Screen grid thickness measurements can be made through the Accel grid, alleviating the need to dismantle the grid set, as the carbon Accel grid is invisible to the X-ray bombardment. This is a very significant advance since any thrust vector evolution due to grid erosion is not masked by changes in the relative grid alignment and exactly the same grid system design can be employed on the EQM and the flight units. It is not practical however to employ the X-ray and WLI techniques at each aperture location. As a consequence these techniques will be

employed at the positions indicated in Figure 31. Note that an aperture numbering convention has been instigated since the measurements must be performed w.r.t. these apertures. This is because in the case of the X-ray diagnostic the grid assembly must be aligned visually. In the case of the WLI the X,Y,Z traverse mechanisms are insufficient to cross the grid dimensions. ***Figure 32*** shows the Hiltonbrooks X-ray generator and Laue camera including the control electronics, detector counting electronics system with PC read-out and laser alignment system.

Figure 32 X-ray absorption machine with screen grid in place for measurement

Figure 33 shows the results of the WLI from the EQM T6 following the initial assembly of the gridset, i.e. 0 hours of operation. Note that the markings on the downstream surface of the Accel grid are the original machining marks from the rolled molybdenum manufacturing process.

The surface topology measurements of the Accel grid (on the downstream concave face of the Accel grid) will be made in the same locations. It is currently planned to employ the WLI for this but the technique fundamentally relies on reflected light. As the grids erode and the surface becomes contaminated with graphite debris the measurements may become unviable. In this case the CMM may be employed.

After the surface topology of the Screen and Accel grids and the Screen grid thickness measurements have been made, the Accel grid aperture bores will be measured using the in-house CMM to determine the bore erosion.

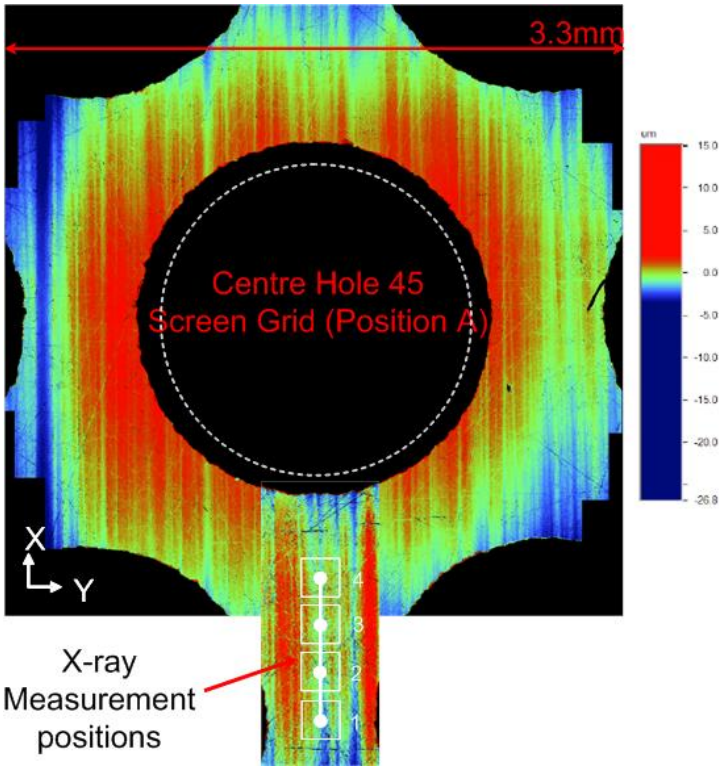

Figure 33 WLI measurements of BepiColombo EQM SEPT Screen Grid (0 Hours)

EOL Grid Manufacture and Testing

An EOL Accel and Screen grid set will be manufactured to reproduce the predictions provided by the 3D ion optics code for end of mission conditions plus qualification margin. This grid set will then be employed for SEPT performance verification testing as part of the EOL TCF test campaign.

The manufacture of the Accel grid is relatively straightforward following the approach previously employed by QinetiQ during the Grid TRP programme. The grid is machined from solid and hence can be directly machined to the surface profile and aperture dimensions predicted by the modeling activities.

IV. Test Facilities Preparation for EMC and Coupling Test

A. EMC testing of the EQM T6 SEPT and QinetiQ's EMC Facility

The EMC/EMI qualification of the SEPT will be performed by operating a thruster inside an RF transparent section of a vacuum chamber. This section will be enclosed within a temporary anechoic screened room. The thruster will be powered using an EQM PPU and a fully flight representative harness.

The aim is to use a fully representative power supply for the EMC tests because the plasma generated by the thruster will respond to any current or voltage transients injected by the power supply. This is also true in reverse; i.e. the power supply will try to respond to any load transients produced by the thruster, therefore a further EMC test on the PPU will be performed whilst coupled to the SEPT. It is, therefore, essential that the power supply responds in a representative manner. Since much of the radiated emissions will originate from fluctuating currents in the intermediate harness connecting the power supply and thruster it is also essential that the harness design, cable screening, connectors, terminations etc. are fully representative, and this is taken into consideration in the test set-up.

QinetiQ's EMC facility (1.7m [D] x 7.5m [L], with the GRP section 3m in length) consists of a 4 m × 3 m × 3 m damped screened enclosure around the RF transparent section of LEEP1 vacuum chamber. It is constructed from bolt-together GRP sections. The Anechoic room is lined with mu-copper foil (0.12 mm thick) which has a better than 100 dB attenuation (200 kHz to 10 GHz).

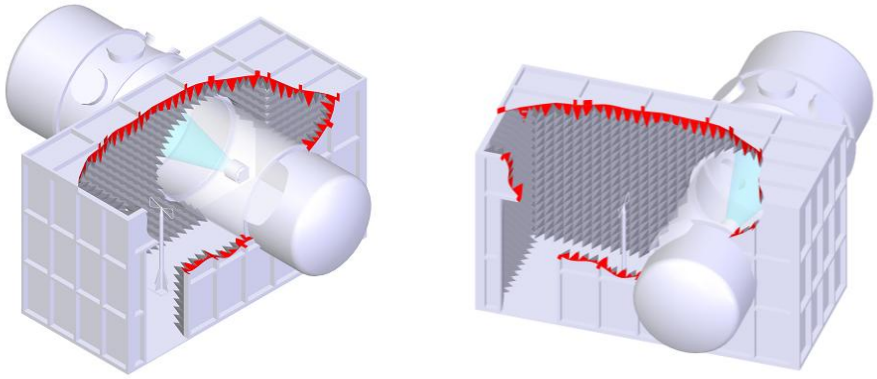

Figure 34 EMC Facility Model

The anechoic chamber is primarily designed for undertaking thruster RF emission measurements over the frequency range 30 MHz to 40 GHz and would also be used to explore thruster susceptibilities to RF emissions from external sources. A schematic is shown in ***Figure 35*** with a test set-up shown in ***Figure 36***. The thruster is mounted from the top of the facility via a composite RF transparent support frame. The Antenna that is located in the Anechoic room, is able to measure RF emissions from the thruster from a number of acute angles typically in the range of 45 degrees from the normal to the beam towards the rear of the thruster. This angle is only limited due to the physical constraints of the facility and anechoic room. It has been deemed unrepresentative to attempt to locate the antenna inside of the vacuum facility for obvious reflection reasons.

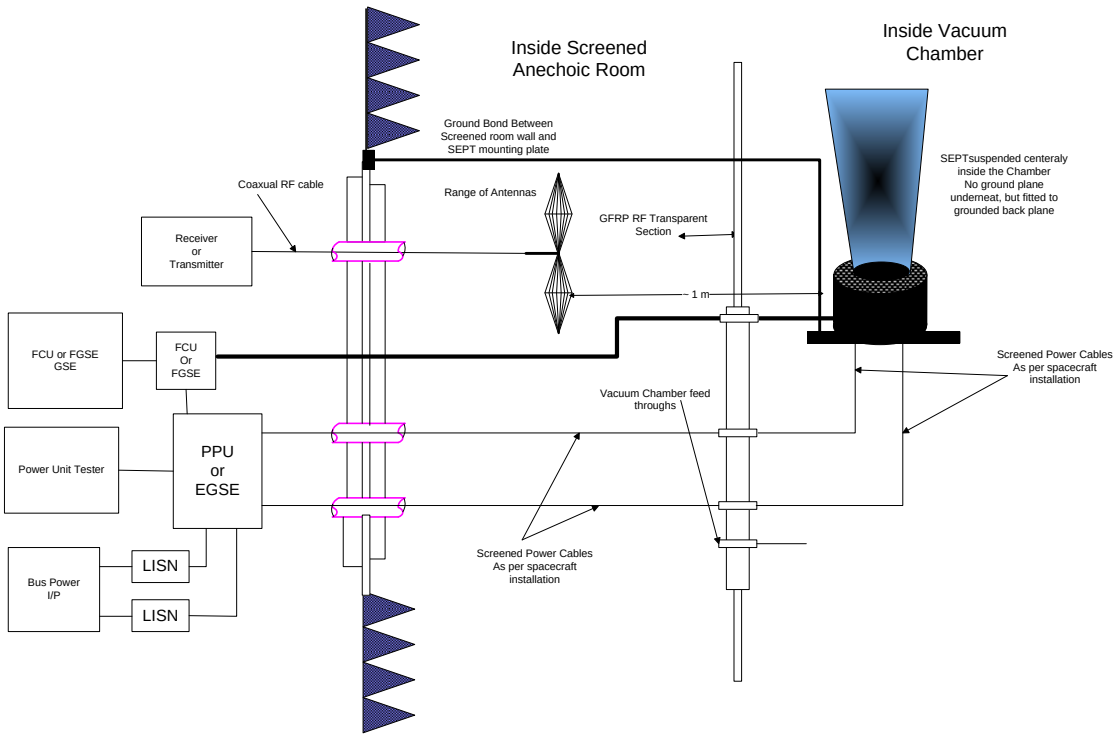

Figure 35 Schematic of SEPS EMC Set-Up showing RF EGSE

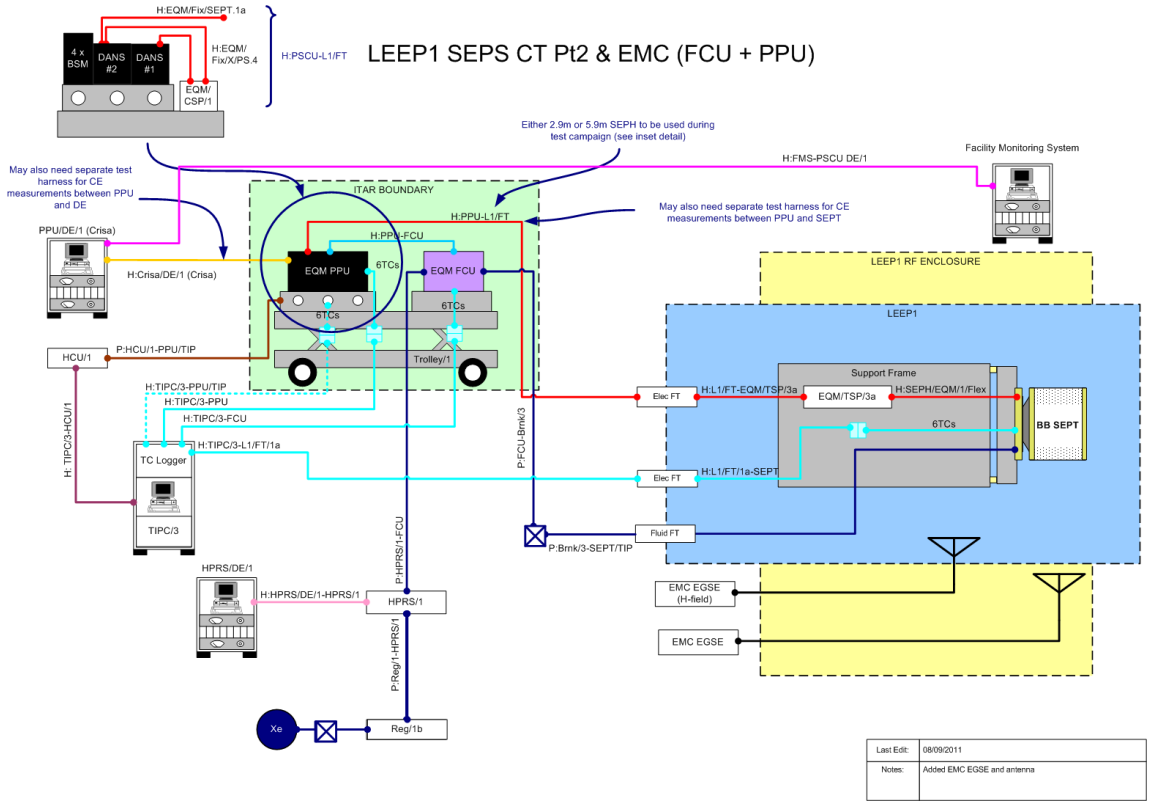

Figure 36 Schematic of SEPS EMC Set-Up showing thruster EGSE

A series of tests to optimize and characterize the RF properties is proposed prior to commencement of the EMC test campaign, which are highlighted below:-

Phase 1

- Optimize position of RF absorbing material (RAM)
- Measure received RF levels in the enclosure from a transmitter at the SEPT location in the vacuum chamber

Phase 2

- Measure RF attenuation of the GRP across the frequency range 30 MHz to 40 GHz vacuum chamber section wall
- Use results to correct the later RF emission measurements from SEPT

Phase 3

- Measure background RF levels to determine enclosure screening effectiveness
- Measure with vacuum chamber sealed, but ancillary equipment (pumps, sensors etc.) switched off
- Measured over a whole day to capture any significant temporal variations that may occur
- Measure with all equipment necessary to keep chamber at operating vacuum pressure – determines their RF interference contribution

Figure 37 shows the EMC facility in its current state at QinetiQ Farnborough.

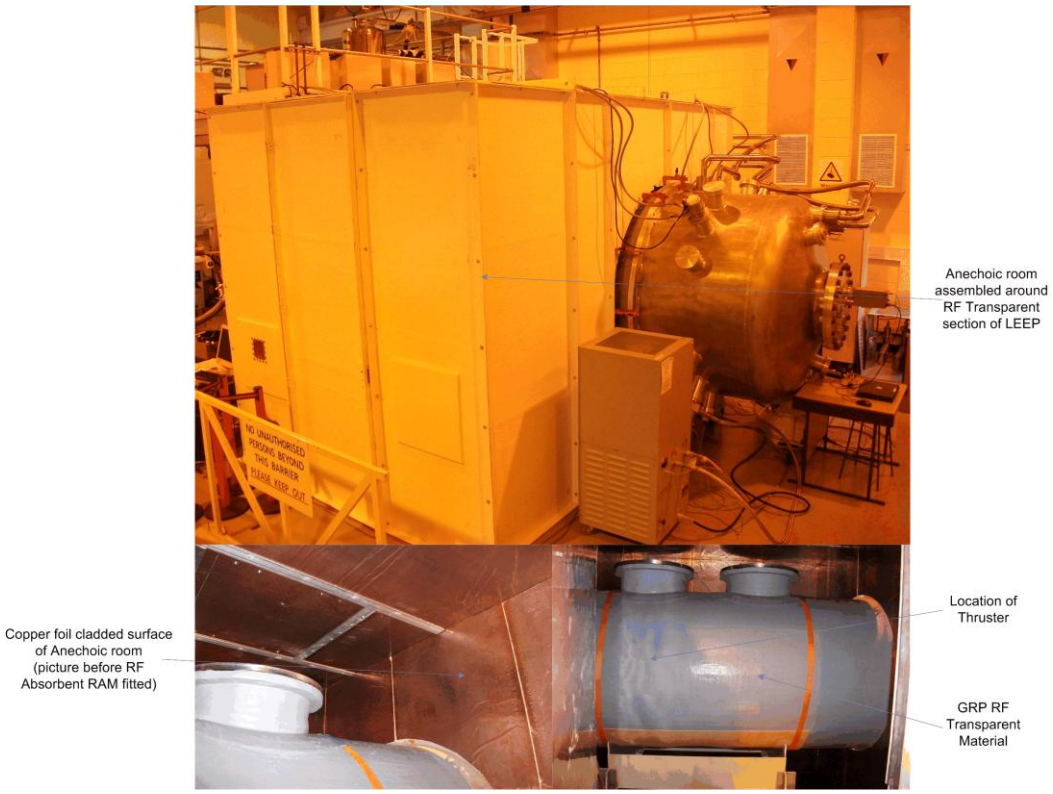

Figure 37 Images of the QinetiQ EMC EP Test Facility

B. Coupling Test Facility

LEEP3 (Large European Electric Propulsion Facility 3) is a new facility that has been manufactured specifically for EP technologies, and will be used for SEPS system testing and Flight Acceptance testing on the BepiColombo programme. Figure 38 and Figure 39 show the facility, chevron graphite target and the external mobile clean room that will accommodate the other SEPS hardware (i.e. PPU and FCU) during the SEPS coupling test campaigns.

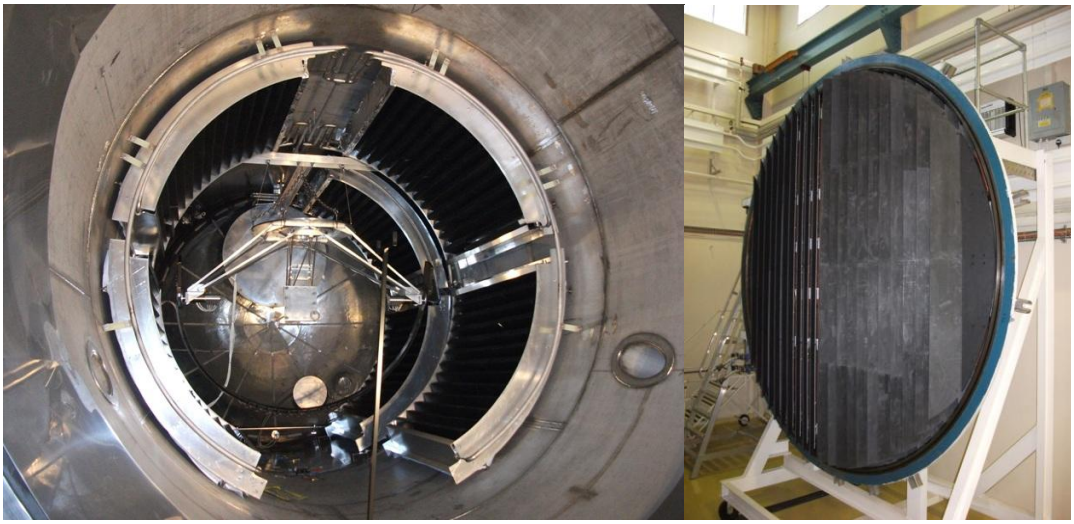

Figure 38 Photograph of LEEP3 (left) with graphite chevron water cooled target (right)

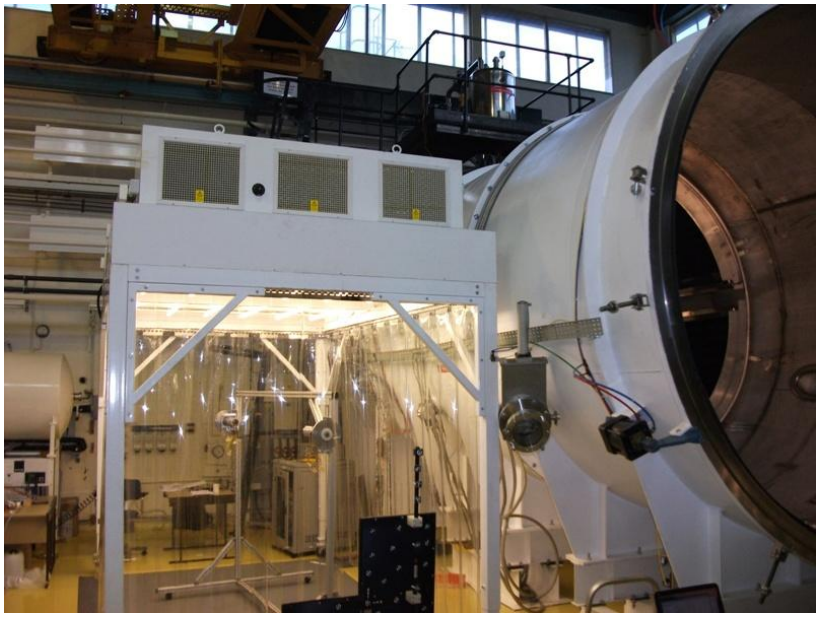

Figure 39 Photograph of LEEP3 and Clean Tent to accommodate SEPS hardware

The LEEP3 facility consists of the following:-

- Interchangeable interface to accommodate either the LEEP2 thrust balance or Invar Thermal Support Frame
- Identical Hemispherical beam probe arm and Faraday cups to LEEP2
- Water Cooled Graphite Chevron Target to minimize backsputter

- 3.3m Diameter x 7.2m Length
- 3 x Sumitomo Cold Heads (RDK400B), Compressors (F50)
- 3 x Leybold Cold Heads (120T), Compressors (Coolpak 6000)
- 1 x Sumitomo Cold Head (FS242), Compressors (F70)
- 1 x CTI Cold Heads (1050CP), Compressors (8500)
- Screwline SP630 Dry Pump + Booster
- Vacuum level achieved 5.0 x 10^{-7} mbar (9.0 x 10^{-6}mabr with flow rate equivalent to single T6 @ 145mN)

V. Conclusion

The respective system architectures for BepiColombo has been described together with the qualification programmes underway. The approach to qualification of the SEPT has been described, as developed through Assembly, Integration and Verification (AIV) activities leading up to the BepiColombo mission, including; mechanical integrity, Thermal Vacuum (TV), Electromagnetic Compatibility (EMC), Electromagnetic Interference (EMI) and thrust performance characterisation as well as the development of the necessary Ground Support Equipment (GSE). Performance verification of a fully representative SEPS is considered to be an essential element in the qualification of the SEPT. The SEPS required for inter-planetary cruise for the ESA BepiColombo mission to the planet Mercury benefits from its wide operating range, robust design and its ability to be easily adaptable to a wide range of platforms and applications. Critical to the SEPS system design is the redundancy and cross-strapping philosophy. The selected configuration of two PPUs with fully symmetric cross-strapping of T6 units to PPU outputs gains maximum benefit from the symmetry of the four engine configuration. The resulting design provides for an elegant AIV sequence and plan. The number of PPU units is minimized and mounting/demounting units is straightforward and the number of operating modes for testing and characterization is minimized.

References

[1] Novara, M, "The BepiColombo ESA Cornerstone Mission to Mercury", IAF Paper IAF-01-Q.2.02, 2001.

[2] Wallace, N, and Fehringer, M, "The ESA GOCE mission and the T5 ion propulsion assembly", IEPC Paper 09-269, 2009.